

# Micro-arc Oxidation (MAO) Coupling Electrophoresis Deposition (EPD) Versus Hydroxyapatite Coating in Periimplantitis: An Experimental Study in Dog

Chuanhua Li<sup>1\*</sup>, Zhifeng Wang<sup>2\*</sup>, Lina Zhu<sup>2</sup>, Dan Hao<sup>1</sup>, Jing Lan<sup>1</sup>

<sup>1</sup>Department of Prosthodontics, Dental School, Shandong University, Jinan City, Shandong Province, China.

<sup>2</sup>Department of Pediatrics Dentistry, Dental School, Shandong University, Jinan City, Shandong Province, China.

## Abstract

**Object:** This paper aims to evaluate the influence of dental implants coated with hydroxyapatite (HA) and implants processed by micro-arc oxidation (MAO) coupling electrophoresis deposition (EPD) on experimental peri-implantitis in Beagle dogs. **Methods:** The thirty-six implants (diameter 3.3 mm & length 11 mm) were equally divided into three groups. Group A was processed with a plasma-sprayed layer of HA, group B was surfaced with MAO and EPD, and group C was not-treated. The morphological surface characteristics and the surfaces chemical composition were observed by scanning electron microscopy (SEM) and energy-dispersive X-ray spectroscopy (EDS). These implants were randomly placed into the alveolar bone of mandible of dogs. After three months (healing stage), cotton ligatures with *P. gingivalis* (strain ATCC 33277) were replaced in the submarginal position around the neck of the implants to induce peri-implantitis. Clinical measurements, including peri-implant probing pocket depth (peri-implant PD), and bleeding on the probing were recorded every 2 weeks during subsequent six weeks. After the animals were euthanized, implants and surrounding tissues were retrieved. The length of bone loss (BLL) was measured. Result: The BLL of group A ( $4.66 \pm 0.22$ ) was higher than that of group B ( $4.04 \pm 0.29$ ), but it was lower than that of group C ( $5.08 \pm 0.28$ ). The difference was statistically significant ( $P < 0.05$ ). Conclusion: Dental implants with MAO coupled with EPD could be more effective for slowing down peri-implantitis progression than HA-coated implants and not-treated implants.

**Key Words:** Peri-implantitis, Hydroxyapatite coating, Plasma spraying, Micro-arc oxidation, Electrophoresis deposition

## Introduction

Due to their excellent biocompatibility and prominent mechanical and corrosion resistance, titanium and its alloys are commonly used as implant materials [1-3]. During the complex process of bone formation at the implant-tissue interface, the roughness of surface and ingredients of implant are important factors for regulating osteoblastic function. Compared with an untreated or smooth surface, higher osteoblast activity is observed in the microstructure of the implant surface (from 1- to 100- $\mu\text{m}$  surface roughness) [4]. Grit blasting treatment roughens the surface of titanium, and thermo-chemical (TCh) treatment forms a bioactive surface and facilitates the development of a bioactive interface. A rough and bioactive-titanium surface obtained by rough-bioactive treatment can enhance the adhesion and differentiation activity of human osteoblasts cells [5] as well as osseointegration [6].

Calcium phosphate minerals on the implants surface, such as apatite, can enhance implant-bone osseointegration at an early stage [7]. Hydroxyapatite (HA) is a compound of calcium and phosphorus, a type of ceramic materials. HA can be generated naturally or be manufactured synthetically. Implants with HA coating present with higher osteoblastic activity and better osteoconductivity than pure titanium implants both in vitro and in vivo [8-11], which can chemically bond to bone tissues [12]. HA coating reduces or even inhibits the release of metal ions into the surrounding tissue [13] and it acts as connective tissue encapsulation around the implant to avoid peri-implant bone apposition [14]. Many techniques can incorporate HA into the layer of titanium oxide, such as deposition in a vacuum environment (e.g., physical vapor

deposition, chemical vapor deposition, and ion beam-assisted deposition), in an air atmosphere (e.g., plasma spraying and laser deposition) and in a solution or suspension (e.g., sol-gel, dip coating, electrochemical or electrophoretic deposition) [15,16].

Titanium plasma spraying (TPS) is one of the most common methods for creating HA-coating. HA powder is heated to an extremely high temperature and projected at a high velocity onto the titanium surface. Then, the particles fuse together and form films that are approximately 40-100 $\mu\text{m}$  thick. Its deposition efficiency can be controlled according to different application requests, such as the morphology and chemical composition of the surface, which is the prominent characteristic [17]. However, the demand of the purity of the gas demand is higher. It is difficult to spray the coating when the diameter of the surface hole is extremely small [18].

Micro-arc oxidation (MAO) is another common method for modifying the implant surface. It is typically characterized by the phenomenon of electrical discharge on the anode in the aqueous solution and a plasma-assisted electrochemical method that produces rough, thick, and porous oxide films on metal surfaces. The local temperature of the metal surface reaches up to 2000 – 5000°C and then slowly cools down. The anneal process of metal substrate and oxide films can be easily observed [19-22]. The stress between the substrate and film is then removed, which prevents the oxide films from falling off from metal substrate. Good quality coatings with high micro-hardness, adhesion strength, and wear resistance are synthesized on the metal surface with MAO technique. Ca and P can be incorporated into the oxide coating with the

MAO technique and combine a variety of compounds, such as  $\text{CaTiO}_3$ ,  $\alpha\text{-Ca}_3(\text{PO}_4)_2$ ,  $\beta\text{-Ca}_2\text{PO}_7$ ,  $\text{CaCO}_3$ ,  $\text{CaO}$  or amorphous apatite [23-26].

The electrophoresis deposition (EPD) technique can deposit colloidal particles from a stable suspension onto an oppositely charged substrate through a direct current (DC) electric field. The particles must be electrically charged to conduct film formation. The important task is to identify effective additives for particle charging [27-29]. However, one disadvantage of this technique is the low adhesion between the coating and substrate. Some cracks on the coating surfaces may appear due to shrinkage after the deposit drying process. Recently, MAO coupling with EPD, following SLA, has been widely used to obtain a coating with a 50-100  $\mu\text{m}$  thickness [30].

Peri-implantitis is an inflammatory response surrounding the implants. It affects the tissues around an osseointegrated implant and results in the loss of supporting bone. The risk factors for peri-implantitis include poor oral hygiene, the depth of the peri-implant pocket, implant material and surface roughness, biomechanical overloading and bacterial infection [31]. Beyond these, the surface roughness and surface-free energy parameters may mainly influence their susceptibility to bacterial infection [32,33]. In our previous research, we found that the dental implant with MAO and EPD obtained stronger osseointegration than the implant with HA coating [34]. The purpose of this study is to investigate the influence of these two surface modifications on peri-implantitis in dogs.

## Materials and Methods

### Materials

Thirty-six pure titanium smooth cylindrical BLB implants (diameter 3.3mm & length 11mm, provided by Beijing Leidon Biomaterial Limited Company, China.) were equally divided into three groups. Group A was processed with a plasma-sprayed layer of HA, and group B had surfaces processed by MAO coupling EPD on sandblasted and acid-etched techniques, and group C had no surface treated.

### Scanning electron microscopy (SEM) and energy-dispersive X-ray spectroscopy (EDS)

The morphological surface characteristics of the group A and group B implants were observed by thermal field SEM (Hitachi SU-70, Shenzhen, China) at an accelerating voltage of 20 kV. The implants were performed for SEM following standard procedures. The surfaces chemical composition was determined by the EDS system connected to the SEM. This system was able to detect atoms with an atomic weight equal to or greater than that of boron and allowed for semi-quantitative analysis of the composition of a surface within 1  $\mu\text{m}$  thickness with high lateral resolution.

### Animal surgical procedures

Nine male beagles (provided by the Experimental Animal Centre of Shandong University), 2-3 years old and weighing from 15 to 20 kg, were used in this experiment. General guidelines about the use of animals had been followed and all studies were approved by the Animal Ethical Committee of Shandong University. Before surgery, anesthesia was induced by femoral vein injection of 3% pentobarbital sodium (1mg/kg, JiangSu Heng Rui Pharmacy Factory,

Lianyungang, China). Under anesthesia, the second and the third premolars of the bilateral mandibles were extracted. Implants were placed randomly into four alveolar sockets in each Beagle. After surgery, all dogs were given 80,000 IU of gentamicin sulfate intramuscularly for three consecutive days as a prophylaxis against infection. After three months (healing stage), the cotton ligatures with *P. gingivalis* (strain ATCC 33277) were ligatured around the neck of all implants and were replaced every two weeks during subsequent six weeks [35]. Before ligation, two weeks, four weeks and six weeks after ligation, the peri-implant probing pocket depth (peri-implant PD) and clinical hemorrhage were examined. The results of peri-implant PD is average by using repeated measurement to calibrate it. All animals were injected with an overdose of sodium pentobarbital euthanasia six weeks after ligation. The operations were performed by the same person in order to reduce the error.

### Histologic observation

After the animals were euthanized, implants and surrounding tissues were retrieved and immediately fixed in 10% buffered formalin at 4°C for 7 days. The specimens were dehydrated in graded alcohols from 70% to 100%, infiltrated and embedded in light-cured resin. After that, the specimens were sectioned at a thickness of 50 $\mu\text{m}$  along with the long axis of implants (EXAKT, Germany). Slices were dyed with methylene blue and observed under a microscope (Nikon, SMZ745T, Japan). The length of bone loss (BLL) was measured from the apical marginal level of bone-to-implant contact to implant shoulder at both the buccal and the lingual aspect of the implant in each section (Fig. 1). The BLL was measured by the optical microscope connected with high resolution image viewing system.

### Statistical analysis

Statistical analysis was performed with SPSS 17.0 software (SPSS Inc., Chicago, IL, USA). The BLL data among different groups were reported as the mean  $\pm$  standard deviation (SD), and one way analysis of variance (ANOVA) was used to assess significant differences at a level of  $P < 0.05$ .

## Results

### SEM, EDS and profilometer analysis

The SEM photograph of group A showed the cloud-form microstructure on the surface, which was distributed widely in an irregular way (Figure 2A). A highly porous layer, yet not uniform throughout the surface of group B consisted of small craters with holes in the center. The diameters of the holes varied widely from approximate 5  $\mu\text{m}$  to  $<1 \mu\text{m}$  (Figure 2B). A large, cloud-form microstructure distributes on the surface of group C implant (Fig. 2C). As for the EDS spectra of two surface modification, it was apparent that the peaks of Ca and P could be observed in the spectra of the HA coating in group A (Figure 3), whereas the maximum peak value of titanium could be observed in group B (Figure 4). Group B also incorporated the peak of Ca, P and oxygen, indicating the existence of those elements in the form oxides. Additionally, the ratio of Ca/P in group A was similar to that in group B. Surface microtopographic analysis showed the rougher surface of group A than that of group B.

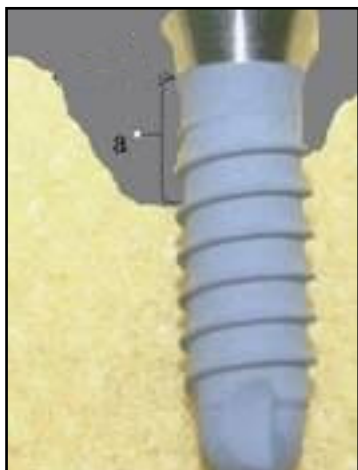


Figure 1: Schematic diagram of vertical bone loss.

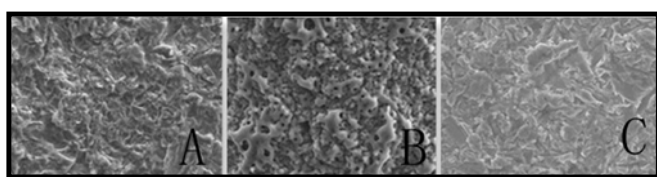


Figure 2: The SEM pictures of the three groups. A: Cloud-form microstructure on the surface of the group A implant, which is distributed widely and densely and irregularly. (magnification×1000). B: The highly porous layer of the group B implant consists of small craters with holes at the center, and is still not yet uniform throughout the surface. (magnification×1000). C: A large cloud-form microstructure distributes on the surface of the group C implant. (magnification×1000).

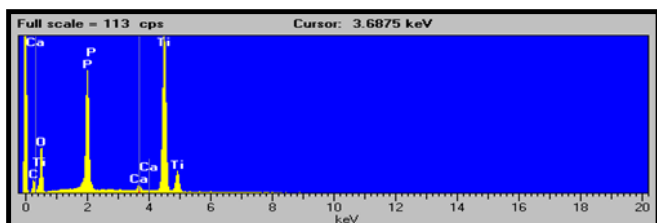


Figure 3. The EDS figure of group A implant. The figure demonstrates the peak of calcium, phosphorous, titanium, and oxygen in the group A implant.

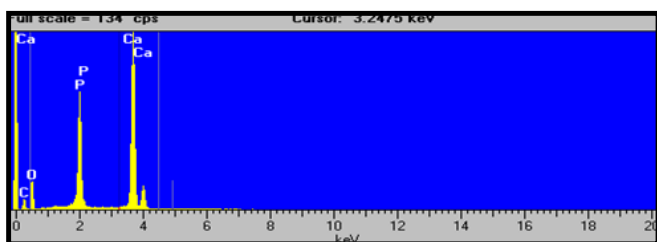


Figure 4. The EDS figure of group B implant. Peaks of calcium and phosphorus can be observed in the spectra of group B, which is compatible with the apatite phase.

**Clinical observations**

No implants were loose during this process. Before ligation, the peri-implant mucosa of each group was similar. The gingival was knife-like, rubbery, and lacking inflammation (Figure 5a). All peri-implant PD values were within the normal range and no significant difference was observed among these groups ( $P>0.05$ ) (Table 1).

At two and four weeks after ligation, oral hygiene deteriorated gradually in all dogs, and soft tissue inflammation was distinctly observed, such as hyperplastic tissues,

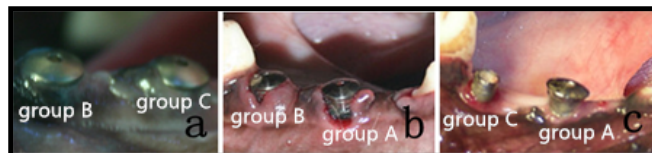


Figure 5. The pictures of implants and gingival tissues. Before ligation, the peri-implant mucosa of each group was similar. The gingival of three groups were knife-like, rubbery, and lacked inflammation (a). Two weeks later, some plaques adhered around all implant necks. Soft tissue inflammation was observed, such as hyperplastic tissue, suppuration, and color changes, which were more severe in group A than in group B (b). Six weeks after ligation, oral hygiene deteriorated, and inflammation of the soft tissues demonstrated obvious differences. Severe pyorrhea was found in group C (c).

Table 1. Peri-implant PD of the three groups at baseline, two weeks, four weeks and six weeks after ligation (mean value ± S.D, n=36) (mm).

Group	Baseline	2 weeks	4 weeks	6 weeks
A	0.76 ± 0.27	3.16 ± 0.29	4.43 ± 0.42	4.07 ± 0.39
B	0.67 ± 0.22	2.98 ± 0.37	4.28 ± 0.39	4.01 ± 0.47
C	0.83 ± 0.32	3.34 ± 0.35	4.56 ± 0.43	4.23 ± 0.45

suppuration, mild clinical hemorrhage and color changes (Figure 5b). Bone loss around the implants was increasingly serious. The values of the peri-implant PD of the three groups had no statistical difference ( $P>0.05$ ), but these data were greater than those measured before ligation (Table 1). At six weeks after ligation, the inflammatory reactions were more severe than before. Severe peripyema and clinical hemorrhage were found in group C (Figure 5c). The gingival recession led decreases in the values of the peri-implant PD (mean=4.01~4.23mm), and there were no statistical difference when comparing three groups (Table 2).

**Histological observation**

In all sections, bone loss was found around every implant and many inflammatory cells were clustered at this area. Furthermore, there were more inflammatory cells in groups A and C than in group B (Figure 6a-c). The bone loss in group A (a) was more severe than that of group B (b), but it was milder than that of group C (c). The HA coating of group A was visualized clearly, and some coatings were fractured or missing at the gingival marginal regions (Figure 7a). There were inflammatory regions between the newly generated bones and implants in group C (Figure 7b). The values of the BLL were shown with the means and standard deviations (mean ± S.D). The BLL of group A ( $4.66 ± 0.22$ ) was higher than that of group B ( $4.04 ± 0.29$ ), but it was lower than that of group C ( $5.08 ± 0.28$ ). The difference was statistically significant ( $P<0.05$ ) (Table 2).

**Discussion**

Dental implants have been valued by an increasing number of doctors and patients to treat dentition defects and edentulous, which are based on the high survival rate for implantation. Both experimental and clinical studies reveal that peri-implantitis is a key factor leading to implant failure, which focus on the impact factors for the dental implantations survival rate [36,37]. Peri-implantitis is an inflammatory process, affecting the tissues around an osseointegrated

**Table 2.** The values of the BLL in the three groups (mean value  $\pm$  S.D, n=36) (mm).

Group	BLL	P value
A	4.66 $\pm$ 0.22	P<0.05
B	4.04 $\pm$ 0.29	
C	5.08 $\pm$ 0.28	

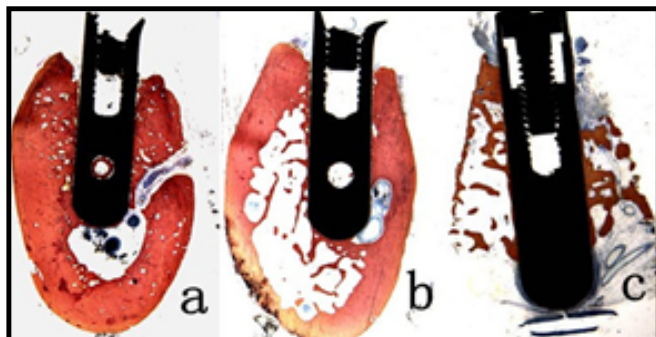


**Figure 6.** The histological pictures of implants and alveolar bone (Magnification  $\times 6.7$ ). The histological picture shows that inflammatory cells were clustered at the bone loss regions. Furthermore, there were more inflammatory cells in groups A (a) and C (c) than group B (b). Bone loss in group A was more severe than that in group B, but it was milder than that of group C (a, b, c).



**Figure 7.** The histological pictures of implants and alveolar bone (Magnification  $\times 20$ ). The HA-coating of group A was visualized clearly and some coatings were fractured or missing at the gingival marginal region (a). There were inflammatory regions between the newly generated bones and implants in group C (b).

implant and resulting in the loss of supporting bone [38]. The risk factors for peri-implantitis include poor oral hygiene, the depth of peri-implant pocket, implant material and surface roughness, biomechanical overloading, bacterial infection and so on [39,40].

In this study, an animal experiment on Beagles was conducted to evaluate the peri-implantitis induced by the dental implants with different surface modifications. We observed that the alveolar bone lost more in implants coated with HA than in implants coated with MAO and EPD, and peri-implantitis of HA coated implants was more serious than that of implants with MAO and EPD, whereas the most serious peri-implantitis happened at untreated implants.

HA coating plays a key role in the initial stages of osseointegration. It not only improves apatite-forming but also increases osteoblast proliferation and differentiation on the implant surface. The formation of apatite on the implant surface is related to its surface structure, composition, and physical and chemical properties [41,42]. Titanium implants coated the HA layer bond to bone chemically, whereas implants without HA coating connect to bone tissue by mechanical interlocking. The HA-coated implants presented with higher osteoconductivity, and attained stronger osseointegration at an earlier stage than the uncoated implants [43]. In the present study, untreated implants had more severe peri-implantitis than HA-coated implants. This stronger osseointegration in HA-coated implants can be favorable to retarding the

progression of inflammation.

Compared with the smooth implant, the rough titanium surface creates a more suitable microenvironment for adhesion, proliferation, and differentiation of the osteoblast towards a mature phenotype [44]. The roughened implants obtain a larger bone-to-implant contact area and higher resistance to torque removal than smooth surface implants [45]. Buser et al. have observed that the contact percentage of the bone-to-implant is enhanced directly through increasing the roughness of the titanium implant [46]. In our study, in spite of the larger surface roughness in the HA-coated implants, the majority of the pit scattering on the surface of the implant modified the MAO and EPD with a diameter of 3–5  $\mu\text{m}$ . The surface coated with MAO and EPD has been identified as the optimal characteristic for implant surfaces [47,48]. More severe peri-implantitis can be observed in group A than in group B because the roughened surface can encourage bacterial adhesion due to the increasing surface area. Hence, the anti-adhesion surface for bacteria is extremely important to prevent implant failure [49]. Amoroso PF et al. report that there is a significant difference in the very smooth (Ra: 34.57 nm  $\pm$  5.79 nm) titanium samples and other samples (Ra: 155 nm  $\pm$  33.36 nm; 223.24 nm  $\pm$  9.86 nm; 449.42 nm  $\pm$  32.97 nm) for the adhesion of *P. gingivalis*. However, there is no significant difference among the other groups except the very smooth group [50]. Bacteria adhesion and proliferation to the implant surface initiate peri-implant infection, which ultimately lead to implant failure [51]. *P. gingivalis* is reported to be a significant component of the predominant microflora around failing implants [52]. In this study, ligatures with *P. gingivalis* ATCC 33277 are placed around the neck of the implants, and peri-implantitis occurs at two weeks after ligation.

A porous, rough, and firmly adherent titanium oxide film on the titanium surface can be produced with the MAO technique [53-55]. The porous coating layer strengthens the anchorage of the implant to the bone [56,57]. MAO replaces the Faraday area in electrochemical oxidation with a high-voltage spark and induces the Ca and P ions in the aqueous electrolytic bath. MAO contributes to the formation of the coating layer composed of Ca and P, which further enhances the bonding between the implant and bone with anchorage.

As for HA-coating, plasma spraying is a commonly used technique, although there are many drawbacks to thermal decomposition and fractures in coating that is more than 40  $\mu\text{m}$ -thick. In this study, we observed that there was several coating flaking and peeling around the HA-coated implants under light microscopy, which does not occur in the implants processed with MAO and EPD. Furthermore, the fractures of HA around the implants are filled with bacteria and leucocytes, which accelerate the loss of alveolar bone. Jovanovic et al. demonstrated that peri-implantitis that is induced by microorganisms is more serious in HA-coated implants than other implants [58]. This may be attributed to the pH variation during the inflammation process, which is induced by phagocyte and microbial decomposition [59].

Surface modification techniques can influence the characteristics of implants. In this study, peri-implantitis is the most serious for the cases with untreated implants. Both HA coating and MAO coupled with EPD surface modification are

useful methods for retarding inflammation progression, and the latter was more effective than the former.

### Conclusions

Dental implants with MAO coupled with EPD could be more effective for slowing down peri-implantitis progression than HA-coated implants and not-treated implants.

### Acknowledgement

The authors report no financial relationship with any

commercial firm that may pose a conflict of interest for this study. No grants, equipment, or other sources of support were provided. The authors report no conflicts of interest related to this study. This work was funded by National Natural Science Foundation of China 30801308 (Beijing, China), Foundation of Department of Science and Technology of Shandong Province 2010G0020237 (Jinan, China), Independent and Innovative Foundation of Shandong University 2012JC010 and 2012TS096 (Jinan, China), Science and Technology of Jinan City(201003143), and Independent and Innovative Foundation of Jinan City(201303039).

### References

1. Das K, Bose S, Bandyopadhyay A, Karandikar B, Gibbins BL. Surface coatings for improvement of bone cell materials and antimicrobial activities of Ti implants. *Journal of Biomedical Materials Research Part B*. 2008; **87**: 455–460.
2. Burns K, Yao C, Webster TJ. Increased chondrocyte adhesion on nanotubular anodized titanium. *Journal of Biomedical Materials Research Part A*. 2008; **88**: 561–568.
3. Narayanan R, Kwon TY, Kim KH. TiO<sub>2</sub> nanotubes from stirred glycerol/NH<sub>4</sub>F electrolyte: Roughness, wetting behavior and adhesion for implant applications. *Materials Chemistry and Physics*. 2009; **117**: 460–464.
4. Fujibayashi S, Neo M, Kim HM, Kokubo T, Nakamura T. Osteoinduction of porous bioactive titanium metal. *Biomaterials*. 2004; **25**: 443–450.
5. Aparicio C, Gil FJ, Planell JA, Engel E. Human-osteoblast proliferation and differentiation on grit-blasted and bioactive titanium for dental applications. *Journal of Materials Science: Materials in Medicine*. 2002; **13**: 1105–1111.
6. C Aparicio, FJ Gil, U Thams, F Muñoz, A Padrós, Josep A Planell. Osseointegration of grit-blasted and bioactive titanium implants: histomorphometry in minipigs. *Key Engineering Materials*. 2004; **254-256**: 737–740.
7. Xu L, Pan F, Yu G, Yang L, Zhang E, Yang K. In vitro and in vivo evaluation of the surface bioactivity of a calcium phosphate coated magnesium alloy. *Biomaterials*. 2009; **30**: 1512–1523.
8. Han Y, Yan Y, Lu C, Zhang Y, Xu K. Bioactivity and osteoblast response of the micro-arc oxidized zirconia film. *Journal of Biomedical Materials Research Part A*. 2009; **88**: 117–127.
9. Huang Y, Wang Y, Ning C, et al. Hydroxyapatite coatings produced on commercially pure titanium by micro-arc oxidation. *Biomedical Materials*. 2007; **2**: 196–201.
10. Kim DY, Kim M, Kim HE, Koh YH, Kim HW, Jang JH. Formation of hydroxyapatite within porous TiO<sub>2</sub> layer by micro-arc oxidation coupled with electrophoretic deposition. *Acta Biomaterialia*. 2009; **5**: 2196–2205.
11. Yao ZQ, Yu. Ivanisenko, T Diemant, A Caron, A Chuvilin, JZ Jiang, RZ Valiev, M Qi, HJ Fecht. Synthesis and properties of hydroxyapatite-containing porous titania coating on ultrafine-grained titanium by micro-arc oxidation. *Acta Biomaterialia*. 2010; **6**: 2816–2825.
12. Le Guéhennec L, Soueidan A, Layrolle P, Amouriq Y. Surface treatments of titanium dental implants for rapid osseointegration. *Dental Materials*. 2007; **23**: 844–854.
13. Browne M, Gregson PJ. Effect of mechanical surface pretreatment on metal ion release. *Biomaterials*. 2000; **21**: 385–392.
14. Upasani VV, Farnsworth CL, Tomlinson T, Chambers RC, Tsutsui S, Slivka MA, Mahar AT, Newton PO. Pedicle screw surface coatings improve fixation in nonfusion spinal constructs. *Spine (Phila Pa 1976)*. 2009; **34**: 335–343.
15. Mach J, Šamoril T, Kolibal M, Zlámál J, Voborny S, Bartošik M, Šikola T. Optimization of ion-atomic beam source for deposition of GaN ultrathin films. *Review of Scientific Instruments*. 2014; **85**: 083302.
16. Vasanthan A, Kim H, Drukteinis S, Lacefield W. Implant surface modification using laser guided coatings: in vitro comparison of mechanical properties. *Journal of Prosthodontics*. 2008; **17**: 357–364.
17. Inaqaki M, Kameyama T. Phase transformation of plasma-sprayed hydroxyapatite coating with preferred crystalline orientation. *Biomaterials*. 2007; **28**: 2923–2931.
18. Liao Xiangling, Tian Weidong, Sui Jing, Yin Peng, Shi Shumin, Wu Bin, Ding Nan. A clinic application and evaluation of short-term results on BLB implant system. *Chinese Journal of Oral Implantology*. 2007; **12**: 73–75.
19. Chen HT, Hsiao CH, Long HY, Chung CJ, Tang CH, Chen CK, He JL. Micro-arc oxidation of b-titanium alloy: Structural characterization and osteoblast compatibility. *Surface and Coatings Technology*. 2009; **204**: 1126–1131.
20. Li J, Wan L, Feng J. Micro arc oxidation of S-containing TiO<sub>2</sub> films by sulfur bearing electrolytes. *Journal of Materials Processing Technology*. 2009; **209**: 762–766.
21. He J, Cai QZ, Ji YG, Luo HH, Li DJ, Yu B. Influence of fluorine on the structure and photocatalytic activity of TiO<sub>2</sub> film prepared in tungstate-electrolyte via micro-arc oxidation. *Journal of Alloys and Compounds*. 2009; **482**: 476–481.
22. Song WH, Ryu HS, Hong SH. Antibacterial properties of Ag (or Pt)-containing calcium phosphate coatings formed by micro-arc oxidation. *Journal of Biomedical Materials Research Part A*. 2009; **88**: 246–254.
23. Deng F, Zhang W, Zhang P, Liu C, Ling J. Improvement in the morphology of micro-arc oxidized titanium surfaces: A new process to increase osteoblast response. *Materials Science and Engineering: C*. 2010; **30**: 141–147.
24. Il Song Park, Min Ho Lee, Tae Sung Bae, Kyeong Won Seo. Effects of anodic oxidation parameters on a modified titanium surface. *Journal of Biomedical Materials Research Part B*. 2008; **84**: 422–429.
25. Li Y, Lee IS, Cui FZ, Choi SH. The biocompatibility of nanostructured calcium phosphate coated on micro-arc oxidized titanium. *Biomaterials*. 2008; **29**: 2025–2032.
26. E Matykina, R Arrabal, P Skeldon. Transmission electron microscopy of coatings formed by plasma electrolytic oxidation of titanium. *Acta Biomaterialia*. 2009; **5**: 1356–1366.

27. Boccaccini AR, Keim S, Ma R, Li Y, Zhitomirsky I. Electrophoretic deposition of biomaterials. *Journal of The Royal Society Interface*. 2010; Suppl 5: S581-613.
28. Javidi M, Javadpour S, Bahrololoom ME, Ma J. Electrophoretic deposition of natural hydroxyapatite on medical grade 316L stainless steel. *Materials Science and Engineering: C*. 2008; **28**: 1509–1515.
29. Wu ZS, Pei S, Ren W, Tang D, Gao L, Liu B, Li F, Liu C, Cheng HM. Field emission of single-layer graphene films prepared by electrophoretic deposition. *Advanced Materials*. 2009; **21**: 1–5.
30. Kim DY, Kim M, Kim HE, Koh YH, Kim HW, Jang JH. Formation of hydroxyapatite within porous TiO<sub>2</sub> layer by micro-arc oxidation coupled with electrophoretic deposition. *Acta Biomaterialia*. 2009; **5**: 2196–2205.
31. Quirynen M, De Soete M, van Steenberghe D. Infectious risks for oral implants: a review of the literature. *Clinical Oral Implants Research*. 2002; **13**: 1-19.
32. Scarano A, Piattelli M, Caputi S, Favero GA, Piattelli A. Bacterial adhesion on commercially pure titanium and zirconium oxide disks: an in vivo human study. *Journal of Periodontology*. 2004; **75**: 292-296.
33. Harris LG, Tosatti S, Wieland M, Textor M, Richards RG. Staphylococcus aureus adhesion to titanium oxide surfaces coated with non-functionalized and peptide-functionalized poly (L-lysine)-grafted-poly(ethylene glycol) copolymers. *Biomaterials*. 2004; **25**: 4135-4148.
34. Yin K, Wang Z, Fan X, Bian Y, Guo J, Lan J. The experimental research on two-generation BLB dental implants - Part I: surface modification and osseointegration. *Clinical Oral Implants Research*. 2012; **23**: 846-852.
35. Fan X, Wang Z, Ji P, Bian Y, Lan J. RgpA DNA Vaccine Induces Antibody Response and Prevents Alveolar Bone Loss in Experimental Peri-implantitis. *Journal of Periodontology*. 2013; **84**: 850-856.
36. Corbella S, Del Fabbro M, Taschieri S, De Siena F, Francetti L. Clinical evaluation of an implant maintenance protocol for the prevention of peri-implant diseases in patients treated with immediately loaded full-arch rehabilitations. *International Journal of Dental Hygiene*. 2011; **9**: 216-222.
37. Chee W. Peri-implant management of patients with aggressive periodontitis. *Journal of the California Dental Association*. 2011; **39**: 416-419.
38. Mombelli A. Etiology, diagnosis, and treatment considerations in peri-implantitis. *Current Opinion in Periodontology*. 1997; **4**: 127-36.
39. Quirynen M, Voqels R. Clinical relevance of surface characteristics on the formation on teeth and implants. *Nederlands Tijdschrift Voor Tandheelkunde*. 2002; **109**: 422-429.
40. Eick S, Markauskaite G, Nietzsche S, Laugisch O, Salvi GE, Sculean A. Effect of photoactivated disinfection with a light-emitting diode on bacterial species and biofilms associated with periodontitis and peri-implantitis. *Photodiagnosis and Photodynamic Therapy*. 2013; **10**: 156-167.
41. Kim HM, Himeno T, Kokubo T, Nakamura T. Process and kinetics of bone-like apatite formation on sintered hydroxyapatite in a simulated body fluid. *Biomaterials*. 2005; **26**: 4366–4373.
42. Wei D, Zhou Y, Yang C. Characteristic, cell response and apatite-induction ability of microarc oxidized TiO<sub>2</sub>-based coating containing P on Ti6Al4V before and after chemical-treatment and dehydration. *Ceramics International*. 2009; **35**: 2545–2554.
43. Stefflik DE, Corpe RS, Young TR, Sisk AL, Parr GR. The biologic tissue responses to uncoated and coated implanted biomaterial. *Advances in Dental Research*. 1999; **13**: 27-33.
44. Mustafa K, Wennerberg A, Wroblewski J, Hulthenby K, Lopez BS, Arvidson K. Determining optimal surface roughness of TiO<sub>2</sub> blasted titanium implant material for attachment, proliferation and differentiation of cells derived from human mandibular alveolar bone. *Clinical Oral Implants Research*. 2001; **12**: 515–525.
45. Becker W, Becker BE, Ricci A, Bahat O, Rosenberg E, Rose LF, Handelsman M, Israelson H. A prospective multicenter clinical trial comparing one- and two-stage titanium screw-shaped fixtures with one-stage plasma-sprayed solid- screw fixtures. *Clinical Implant Dentistry and Related Research*. 2000; **2**: 159-165.
46. Buser D, Schenk RK, Steinemann S, Fiorellini JP, Fox CH, Stich H. Influence of surface characteristics on bone integration of titanium implants. A histomorphometric study in miniature pigs. *Journal of Biomedical Materials Research*. 1991; **25**: 889-902.
47. Albrektsson T, Wennerberg A. Oral implant surfaces: part 2 – review focusing on clinical knowledge of different surfaces. *International Journal of Prosthodontics*. 2004; **17**: 544–564.
48. Shalabi MM, Gortemaker A, Van't Hof MA, Jansen JA, Creugers NH. Implant surface roughness and bone healing: a systematic review. *Journal of Dental Research*. 2006; **85**: 496–500.
49. Wang XJ, Wang GW, Liang J, Cheng J, Ma W, Zhao Y. Staphylococcus aureus adhesion to different implant surface coatings: An in vitro study. *Surface and Coatings Technology*. 2009; **203**: 3454-3458.
50. Amoroso PF, Adams RJ, Waters MG, Williams DW. Titanium surface modification and its effect on the adherence of Porphyromonas gingivalis: an in vitro study. *Clinical Oral Implants Research*. 2006; **17**: 633-637.
51. Abu-Serriah MM, McGowan DA, Moos KF, Bagg J. Extra-oral craniofacial endosseous implants and radiotherapy. *International Journal of Oral and Maxillofacial Surgery*. 2003; **32**: 585-592.
52. Sbordone L, Barone A, Ramaglia L, Ciaglia RN, Iacono VJ. Antimicrobial susceptibility of periodontopathic bacteria associated with failing implants. *Journal of Periodontology*. 1995; **66**: 69-74.
53. Sul YT, Johansson C, Byon E, Albrektsson T. The bone response of oxidized bioactive and non-bioactive Titanium implants. *Biomaterials*. 2005; **26**: 6720–6730.
54. Wang YM, Liang BL, Lei TQ, Guo LX. Microarc oxidation coating formed on Ti<sub>6</sub>Al<sub>4</sub>V in Na<sub>2</sub>SiO<sub>3</sub> system solution: microstructure, mechanical and tribological properties. *Surface Coating Technology*. 2006; **201**: 82–89.
55. Ryu HS, Song WH, Hong SH. Biomimetic apatite induction of P-containing titania formed by micro-arc oxidation before and after hydrothermal treatment. *Surface Coating Technology*. 2008; **202**: 1853–1858.
56. Sun L, Berndt CC, Gross KA, Kucuk A. Material fundamentals and clinical performance of plasma-sprayed hydroxyapatite coatings: a review. *Journal of Biomedical Material Research Part B: Applied Biomaterials*. 2001; **58**: 570–592.
57. Bigi A, Boanini E, Bracci B, Facchini A, Panzavolta S, Segatti F, Sturba L. Nanocrystalline hydroxyapatite coatings on titanium: a new fast biomimetic method. *Biomaterials*. 2005; **26**: 4085–4089.
58. Jovanovic SA, Kenney EB, Carranza FA Jr, Donath K. The regenerative potential of plaque-induced peri-implant bone defects treated by a submerged membrane technique: an experimental study. *The Internal Journal of Oral & Maxillofacial Implants*. 1993; **8**: 13-18.
59. van Blitterswijk CA, Grote JJ, de Groot K, Daems WT,

Kuijpers W. The biological performance of calcium phosphate ceramics in an infected implantation site: I. Biological performance

of hydroxyapatite during *Staphylococcus aureus* infection. *Journal of Biomedical Materials Research*. 1986; 20: 989-1002.